J. Mar. Biol. Ass. U.K. (2004), **84**, 4516/1–19
Printed in the United Kingdom

The spatial distribution of plankton communities in a Slope Water anticyclonic Oceanic eDDY (SWODDY) in the Southern Bay of Biscay

Emilio Fernández*, Florentina Álvarez[†], Ricardo Anadón[†], Susana Barquero[‡], Antonio Bode[‡], Ana García[∫], Carlos García-Soto[∫], Julio Gil[∫], Nicolás González[‡], Arantza Iriarte[5], Beatriz Mouriño*, Francisco Rodríguez[6]***, Ricardo Sánchez[∫], Eva Teira*, Silvia Torres*, Luis Valdés[7], Manuel Varela[‡], Ramiro Varela[1], Manuel Zapata*[6]

*Facultad de Ciencias, Universidad de Vigo, E-36200, Vigo, Spain. [†]Departamento de Biología de Organismos y Sistemas, [‡]Universidad de Oviedo, E-33071, Oviedo, Spain. [‡]Instituto Español de Oceanografía, Centro Costero de A Coruña, E-15001, A Coruña, Spain. [∫]Instituto Español de Oceanografía, Centro Costero de Santander, E-39004, Santander, Spain. [5]Departamento de Biología Vegetal y Ecología, Universidad del Pais Vasco, E-48080, Bilbao, Spain. [6]Centro de Investigacións Mariñas, Xunta de Galicia, E-36620, Vilanova de Arousa, Spain. [7]Instituto Español de Oceanografía, Centro Costero de Gijón, E-33212, Gijón, Spain. *Corresponding author, e-mail adress: esuarez@uvigo.es. **Present adress: Plymouth Marine Laboratory, Prospect Place, West Hoe, PL1 3DH, Plymouth, UK. ***Present adress: Station Biologique, UMR 7127 CNRS/INSU/UPMC, BP 74, 29682 Roscoff (France). ****Present adress: CIACOMAR–Universidade do Algarve, Avenida 16 de Junho s/n. 8700-311 Olhão (Portugal).

Slope Water anticyclonic Oceanic eDDIES (SWODDIES) are typical mesoscale features of open-ocean waters of the Southern Bay of Biscay which usually develop in winter by shedding from the seasonal poleward current flowing along the northern Spanish slope. These eddies have been intensively studied from the physical perspective. However, their effect on the distribution of biological properties and on the functioning of the pelagic ecosystem has not been assessed so far. To this aim, a sea-truth, multidisciplinary and comprehensive study of a SWODDY was carried out in summer 1998. The eddy, of radius ~50 km, was initially centred at 45.5°N 6.0°W, being characterized by a relatively homogeneous core of water in the centre of the eddy extending from 80 to about 200 dbar. In the central region of the core, temperature (12.55–12.75°C) and salinity (~35.70) values were higher than outside the eddy. The optical properties of the eddy also differed from those of the surrounding waters. A distinct biological signature was found associated with the eddy. Depth-integrated chlorophyll *a* concentrations were 25% higher at the eddy centre where upward doming of the seasonal pycnocline (up to 30 dbar) occurred. Enhanced phytoplankton biomass was related to a higher contribution of $>10\,\mu$m cells, mainly represented by diatoms and chrysophyceans. Phytoplankton and mesozooplankton species composition in and outside the eddy differed significantly reflecting the coastal origin of the water parcel trapped by the eddy. The sharp modification of the planktonic community composition, biomass and associated size-structure caused by slope water oceanic eddies are likely to exert a significant effect upon the upper trophic levels of the pelagic ecosystem of the Southern Bay of Biscay.

INTRODUCTION

Eddy motion in the ocean is a widespread phenomenon mainly generated at regions where strong mean shear flow occurs (Wyrtki et al., 1976). A considerable body of knowledge accumulated during the last decades clearly demonstrated that mesoscale eddy activity exerts a profound effect on the chemistry and biology of open oceanic waters by enhancing productivity and by inducing entrainment and subsequent horizontal advection of planktonic organisms (e.g. The Ring Group, 1981; Angel & Fasham, 1983; Falkwoski et al., 1991; Smith et al., 1996). Eddies transport physical, chemical and biological properties over long distances from the location where they are formed and constitute isolated ecological systems whose function substantially differs from that of the surrounding waters. In recent years, detailed observational and modelling investigations (e.g. McGillicuddy & Robinson, 1997; McGillicuddy et al., 1998; Oschlies & Garçon, 1998; Oschlies et al., 2000; Garçon et al., 2001) have stressed the significant role of eddy dynamics upon the injection of nutrients into the photic layer and, ultimately, on the magnitude of new production in the open ocean.

Maps of eddy kinetic energy for the Atlantic Ocean calculated from surface drift currents derived from merchant ships (Wyrtki et al., 1976) show relatively high mesoscale eddy activity associated with the Bay of Biscay region. Moreover, remote sensing studies based on the analysis of sea surface temperature from infrared imagery displayed a widespread distribution of cyclonic and anticyclonic eddies of small horizontal extent over the Bay of Biscay abyssal plain (Dickson & Hughes, 1981). A similar mesoscale pattern showing the presence of anticyclonic

Table 1. *Physical characteristics of surface (10 dbar) and subsurface waters (200 dbar) at stations located inside (St. 20 and 27) and outside (St. 23 and 31) the slope water oceanic eddy (AE6).*

	St. 20 Eddy centre	St. 27 Eddy centre	St. 23 Outside eddy	St. 31 Outside eddy
Latitude N	45°17	45°17	45°17	45°47
Longitude W	6° 10.50	6° 10.35	6° 53	6° 10.43
Water depth (m)	4250	4800	4400	4800
Depth 12°C isotherm (m)	425	363	251	207
10 dbar				
Potential temp °C	19.49	19.43	19.81	19.75
Salinity	35.809	35.803	35.708	35.818
Sigma-t	25.513	25.523	25.350	25.451
200 dbar				
Potential temp °C	12.42	12.48	12.11	12.01
Salinity	35.697	35.698	35.674	35.665
Sigma-t	27.044	27.032	27.087	27.099

Table 2. *Vertical attenuation coefficients and absorption characteristics (integrated over the 400–700 nm photosynthetically available radiation [PAR] range) of suspended particulate matter for stations located inside (St. 20 and 27) and outside (St. 23 and 31) the slope water oceanic eddy (AE6). Ap (absorption coefficient of total suspended particulate matter), Aph (absorption coefficient of chlorophyll-containing particles), Ad (absorption coefficient of non-phytoplankton particulate matter).*

	St. 20 Eddy centre	St. 27 Eddy centre	St. 23 Outside eddy	St. 31 Outside eddy
Ap 5 m	5.0	1.9	2.1	1.7
Ap 1% Io	11.0	4.7	5.4	3.8
Aph 5 m	4.0	1.4	1.5	1.3
Aph 1% Io	9.1	3.7	4.6	3.2
Ad 5 m	1.0	0.5	0.5	0.4
Ad 1% Io	1.9	1.0	0.9	0.6
Kd (PAR) (m^{-1})	0.056	0.096		0.07
Kd 440/Kd 660	0.307	0.5		0.19

eddies of radius 50–75 km was inferred from sea-truth observations obtained with drifting buoys deployed in the western approaches of the Bay of Biscay (Madelain & Kerut, 1978).

Among the diverse types of eddies described in waters of the Bay of Biscay (Madelain & Kerut, 1978; Pingree & Le Cann, 1992a), the study of Slope Water Oceanic eDDIES, named SWODDIES by Pingree & Le Cann (1992a), has received increasing attention especially from a physical perspective. According to these authors, SWODDIES are anticyclonic parcels of water of radius 50–60 km rotating at maximum velocities of about 30 cm s^{-1} and migrating westward at $\sim$2 cm s^{-1} over extended temporal scales (>9 months). They are characterized by an upper core of water warmer and saltier than the adjacent waters. Remote sensing studies revealed that they are formed in the winter period as they shed from the jet-like current flowing poleward along the upper slopes of the southern Bay of Biscay (Pingree & Le Cann 1990, 1992a, 1992b; Garcia-Soto, 2004). Hydrographic surveys conducted across SWODDIES observed doming of the seasonal pycnocline near the eddy centre resulting in lower sea-surface temperature that allows their monitoring from infrared satellite imagery (Pingree & Le Cann, 1992a, 1992b). A significant surface chlorophyll response associated with the doming of the seasonal thermocline has been recently described (Garcia-Soto et al., 2002; swoddy F90).

Although the current knowledge on SWODDIES is important (see references above), investigations focused on the ecological characteristics of this particular type of eddies have not been conducted so far. However, the observed doming of the seasonal pycnocline with associated increased chlorophyll values, as well as the retention of characteristics of slope waters within the eddy allowed us to hypothesize that measurable differences might be expected in the structure and functioning of the biological communities inhabiting these eddies with respect to surrounding waters of the Bay of Biscay. These presumed changes in ecological properties induced by SWODDIES are likely to be significant for the overall functioning of the pelagic communities in the Southern Bay of Biscay, given the recurrent presence of anticyclonic oceanic eddies over seasonal and interanual scales (see Table 2 in Pingree & Le Cann, 1992a).

To test this hypothesis, a comprehensive, multidisciplinary observational programme (GIGOVI) was designed to examine the relationship between the physical characteristics of SWODDIES and the composition, distribution and functioning of the planktonic food web. Firstly, a monitoring programme of the mesoscale field of the Southern Bay of Biscay using infra-red satellite imagery was initiated ten months earlier and further intensified three months before sea-truth observations took place. A cold core eddy, named AE6, was detected, its evolution monitored, and finally selected for a further detailed study given the thermal and dynamic characteristics which suggested that the feature was probably a SWODDY. Eddy AE6 was then intensively investigated *in situ* during a 20 days cruise.

A detailed account of the remote sensing structure (Advanced Very High Resolution Radiometer [AVHRR], altimeter and SeaWiFS) and mesoscale and submesoscale physical properties of anticyclonic eddy AE6 has been published elsewhere (Garcia-Soto et al., 2002; Sánchez & Gil, in press). In this paper, we present a wider overview of the physical, chemical and biological observations obtained from both the initial remote sensing and the subsequent sea-truth programme conducted in the Southern Bay of Biscay in summer 1998.

Author: quasy-synoptic OK? or quasi-synoptic? (see through-out paper)

MATERIALS AND METHODS

The oceanographic cruise GIGOVI898 was conducted in the Southern Bay of Biscay (45.8°–44.7°N 7.5°–4.7°W) on board RV Professor Shtokman from 12–31 August 1998. A total of 121 conductivity–temperature–depth (CTD) probe stations were visited during the cruise to locate the eddy centre and define its thermohaline structure (Figure 1). The results presented in this paper largely derive from

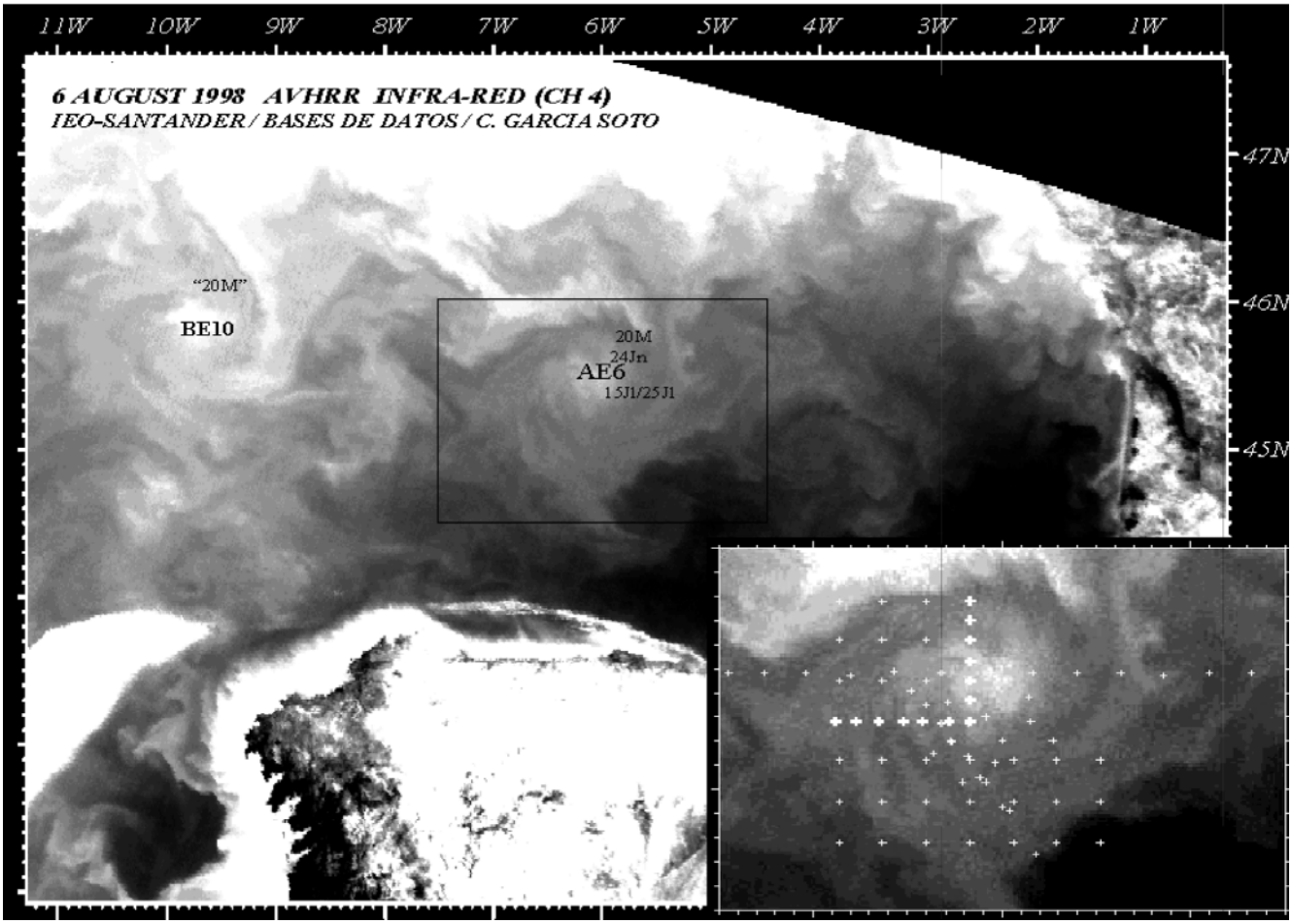

Figure 1. AVHRR thermal infra-red image of the Bay of Biscay on 6 August 1998, 6 days before the beginning of the survey (12–31 August 1998). Capital letters (AE6 and BE10) indicate the central positions of anticyclonic eddies proposed initially for sampling (eddy centres at ~45.5°N 6.0°W and ~45.9°N 9.8°W respectively). The central positions on previous dates are annotated with smaller sized letters, 20M meaning 20 May, 24Jn meaning 24 June, etc. An enlarged image of AE6 is shown in the lower right corner of the Figure. Crosses represent the sampling stations during the cruise, and boldfaced crosses indicate 'biological stations' intensively studied in this paper.

three sampling sections. A N–S quasy-synoptic section crossing through the eddy centre (St. 31 to 60), sampled from 18–22 August and two perpendicular sections visited from 16–18 August (a N–S section running from station 31 to 27 and an E–W section from St. 20 to 23). Separation between stations was ~18 km, except at two high resolution spatial sections where they were ~9 km apart. At 17 selected stations (biological stations), optical properties of the water column, concentrations of nitrate and oxygen, composition and biomass of phytoplankton, bacteria and zooplankton and rates of primary production and net community respiration were also quantified. For the sake of synopticity, only the results derived from 13 of those stations are presented in this paper. Nevertheless, the information obtained in all the biological stations sampled is consistent.

Infra-red satellite images from the AVHRR were used during the study to locate and monitor the evolution of the anticyclonic eddy. The AVHRR sensor is characterized by a radiometric resolution of ~0.12°C in the thermal infra-red band 4 (10.3–11.3 mm) and a spatial resolution (~1.1 km at nadir) suitable to investigate the mesoscale structures of the Biscay region (e.g. Dickson & Hughes, 1981). The AVHRR data were processed as channel 4 images (brightness temperature) following Holligan et al. (1989). Maps of sea level anomaly were also elaborated, after completion of the cruise, using combined TOPEX-Poseidon and ERS-2 data provided by the CLS AGORA and DUACS Projects. The analysis of altimeter data to sea level anomalies follows Le Traon & Ogor (1998), the sea level anomalies are relative to a 3 year mean (January 1993–January 1996) and the instrumental noise is about 2 cm RMS (TOPEX-Poseidon) and 3 cm RMS (ERS-2).

Vertical profiles of temperature, salinity and fluorescence were obtained with a Neil Brown MARK-III CTD probe attached to a rossette (48 casts) provided with 10 litre Niskin bottles and with a Seabird SBE25 CTD system (73 casts). An objective analysis technique similar to that developed by Barnes (1964, 1973) based on a method of successive corrections using normalized weighting functions was applied to obtain the oceanographic field of selected variables. A 3D grid with 5.5×3.9 km horizontal distance between grid points, and vertical resolution 1 m was interpolated from the original dataset. At selected stations, the vertical attenuation coefficient at different wave-lengths was determined with a

LICOR 1800 UW spectroradiometer which was deployed down to 90 m. Subsurface irradiance readings were corrected according to the irradiance values recorded with a LICOR 2π PAR sensor located on-deck.

At every 'biological' station, the concentration of dissolved inorganic nitrate and ammonium was measured with a Technicon AAII autoanalyzer (Grashoff et al., 1983) and the concentration of dissolved oxygen according to the Winkler method (see UNESCO, 1994). Vertical nitrate fluxes across the deep chlorophyll maximum were calculated from the product of the estimated diffusion coefficients Kz and the gradients of nitrate concentration across the deep chlorophyll maximum as detailed in Mouriño et al. (2002).

The concentration of chlorophyll *a* by three phytoplankton size-classes (0.2–2 μm, 2–10 μm and $>10\,\mu$m) were determined fluorimetrically on 90% acetone extracts as described in Teira et al. (2001). The absorption coefficients of total particulate matter (Ap), chlorophyll-containing particles (Aph) and non-phytoplankton particulate matter (Ad) integrated over the 400–700 nm photosynthetically available radiation (PAR) range were determined as in Varela et al. (1998). The concentration of marker pigments were measured by high performance liquid chromatography (HPLC) as detailed in Zapata et al. (2000). The abundance of phytoplankton species was quantified by settling 50–100 ml Lugol-fixed samples. Phytoplankton cells $>2\,\mu$m were counted using an inverted microscope. Size-fractionated primary production rates (0.2–2 μm, 2–10 μm and $>10\,\mu$m) were measured through the incorporation of $NaH^{14}CO_3^-$ during *in situ* simulated incubations of seawater samples collected from five depths as described in Teira et al. (2001). Rates of microbial net O_2 community production were determined from *in vitro* changes in dissolved oxygen after 24 h light and dark incubations as in Serret et al. (1999). Nitrate and ammonium uptake rates were determined experimentally by means of incubations of plankton from three depths within the euphotic zone with tracer amounts of ^{15}N (Dudgale & Goering, 1967; Glibert et al., 1982). New production was estimated from nitrate uptake and f values were computed for selected stations. Daily new production rates were calculated from hourly rates by assuming that N incorporation occurred at the same rate over the 24 h period.

Bacterial abundance was determined in samples preserved with glutaraldehyde (5% final concentration) using the method of Porter & Feig (1980). Bacterial cellular carbon was estimated from biovolumes using the empirical equation of Norland et al. (1987) for bacteria between 0.001 and 0.5 μm^3. Bacterial biovolumes were computed from measurements of bacterial dimensions. Mean biovolume of bacteria in this study was $0.11 \pm 0.09\,\mu m^3$ cell^{-1} (N=254), and the resulting carbon content was 12.7 ± 10.5 fg C cell^{-1}.

A triple WP2 net (40 cm diameter and 200 μm mesh) was used for mesozooplankton sampling (Fraser, 1968). The net was deployed down to 200 m at a speed of 1 m s^{-1}. One of the three samples was sequentially screened through 1000 μm and 200 μm and then both size fractions filtered through glass fibre filters, these were then frozen (-20°C) until the further determination of dry weight ashore. Samples for taxonomic identification of zooplankton were preserved with borax buffered formalin (4%) and the species identified and counted under the stereomicroscope.

RESULTS

Satellite imagery

Figure 1 shows a thermal infra-red image of the Bay of Biscay on 6 August 1998, six days before the beginning of the survey. The surface central region of two anticyclonic eddies (AE6 and BE10) can be seen in the thermal infra-red image as an oval patch of cool water (white shades), known to indicate the local elevation of the seasonal thermocline of SWODDIES (Pingree & Le Cann, 1992a). The anticyclonic sense of rotation of both structures is visualized by filaments of cool water coming from the north ($\sim$46.5°N) that trace the field of flow at the northern and eastern margins of the eddies. Comparison with simultaneous altimeter observations (sea level anomalies) reveals that these jet structures result in surface water being drawn around the eddy margins between the main anticyclone and associated smaller surrounding cyclones (Garcia-Soto et al., 2002). Maps of sea level anomaly (mm) are also shown here (Figure 2) shortly before, during and shortly after the cruise time (12–31 August) and they show the spatial structure of the swoddy AE6 changing in time by interaction with the surrounding cyclones (see for example C1). The anticyclone AE6 was chosen as the target mesoscale structure for sea-truth sampling as the series of satellite observations indicated that it was a persistent feature. AE6 was last observed on 22 September at $\sim$45.3°N 7.0°W having travelled westwards $\sim$100 km since its first AVHRR observation on 20 May. Before 20 May, AVHRR observations of the eddy were scarce due to unsettled weather that made it difficult to track eddies continuously.

Thermohaline structure

The spatial distribution of temperature at the 200 m isobath during the survey clearly shows the presence of a warm, relative to water outside or adjacent to the eddy, subsurface core of water located at the eddy centre and delineates the extension of AE6 (Figure 3). Temperature at 200 dbar changed from 12°C outside the eddy to 12.4°C at the centre, over a horizontal scale of 50–60 km. The thermal gradient established between subsurface waters located outside and inside the eddy (0.04–0.05°C km^{-1}) indicates progressive depression of isotherms towards the eddy centre resulting in anticyclonic motion of the mesoscale structure.

A N–S quasy-synoptic section crossing through the eddy centre (Stations 31 to 60; for reference see Figure 3) shows the presence of the seasonal pycnocline in the upper 70 dbar and the slope of isotherms, isohalines and, hence, isopycnals towards the eddy centre (Figure 4). The section shows a central homogeneous core situated between 80–200 dbar with typical near-constant salinity (35.70) and a weak temperature gradient from 12.75–12.55°C at the eddy centre. The slope of isohalines decreased considerably below the 27.1 isopycnic surface due to the progressive extinction of the core. The core of the eddy was

Author: 35.70? should this be 35.70 psu?

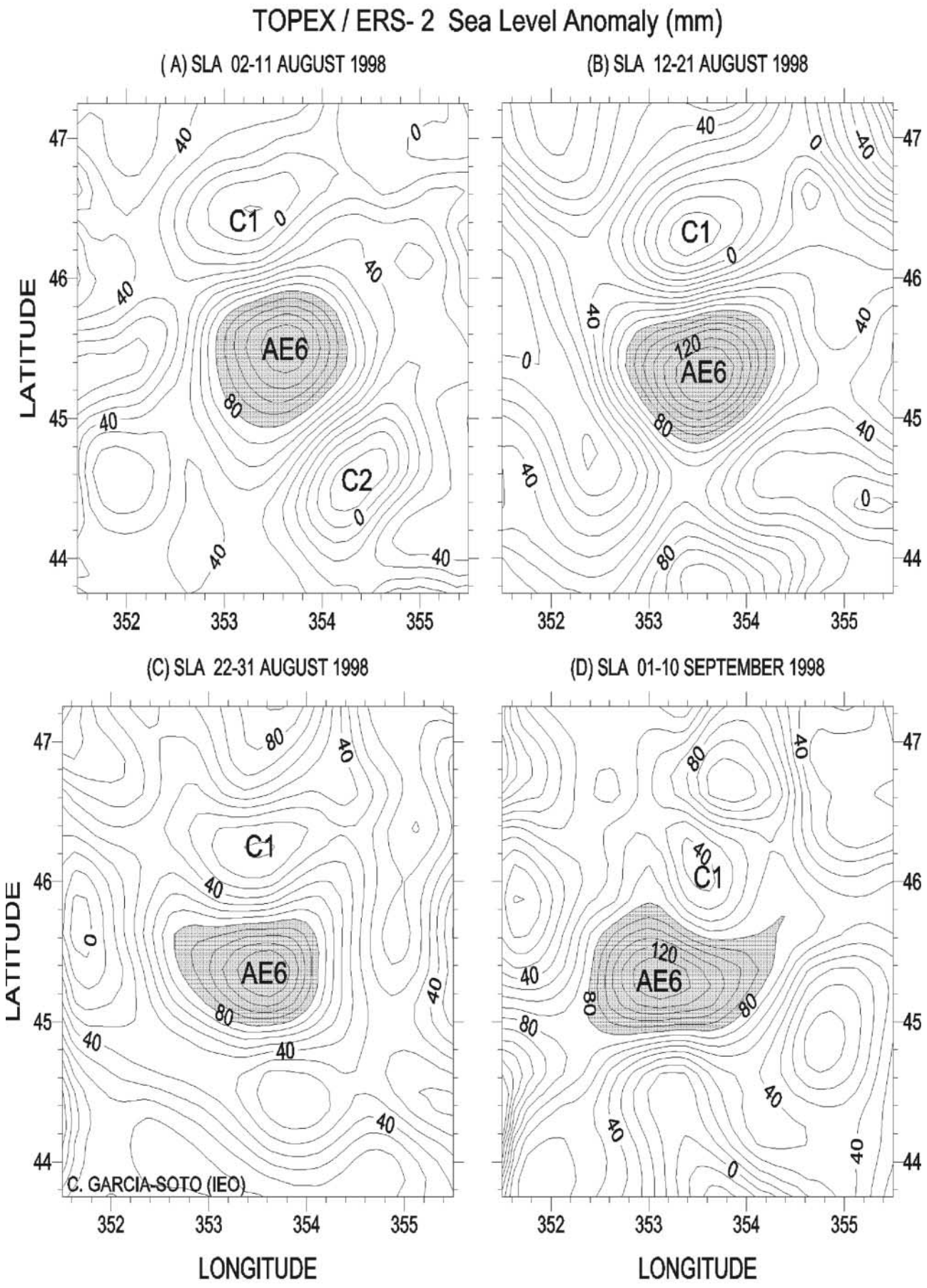

Figure 2. Maps of sea level anomaly (Topex-Poseidon and ERS-2 data) showing the spatial structure of swoddy AE6 on dates: (A) 02–11 August 1998; (B) 12–21 August 1998; (C) 22–31 August 1998 and 01–10 September 1998. The sea level elevation associated to the anticyclonic swoddy is highlighted with shading. 'C1' and 'C2' indicate surrounding cyclones.

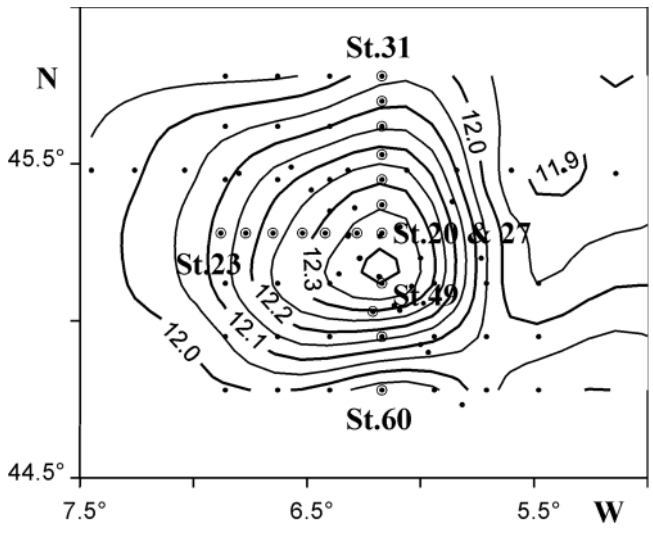

Figure 3. Distribution of temperature (°C) at the 200 m isobath. Dots represent CTD stations. Encircled dots indicate stations included in the sections shown in Figures 4 to 8. The codes of the main stations cited in the text are also shown.

warmer and saltier than neighbouring waters. Typical potential temperature and salinity values at 200 dbars were 12.42–12.48°C and 35.69, respectively (Table 1), values 0.3–0.4°C and 0.02–0.03 higher than those measured in waters located outside the eddy. Sigma-t values at 200 dbar were lower inside the eddy. By contrast, surface waters were cooler, saltier and denser at surface layers of the eddy centre as a consequence of the outcropping of the seasonal pycnocline. The observed density field could somewhat be affected by tidal activity. However, given the fact that several stations were visited in different times within a quasy-synoptic time scale, it seems likely that tidal effects on the quasy-geostrophic adjustment were largely filtered.

Figure 5 represents E–W geostrophic velocities calculated for a high spatial resolution CTD section. 1500 dbar was selected as the no motion level. Velocities were calculated below 65 dbar to overcome the perturbation of the density field caused by internal waves (see Figure 10). The distribution of geostrophic velocities reveal the anticyclonic rotation of the eddy down to 1500 m. Velocities exceeding $>10\,\mathrm{cm\,s^{-1}}$ were found in the upper 300 dbar, $\sim$20 km away from the eddy centre. The geostrophic velocity field at surface layers was asymmetric with higher velocities in the southern region of the section. The interaction of AE6 with mesoscale surface structures appears as the most likely explanation for this geostrophic pattern (Sánchez & Gil, in press). In the northern part of the eddy, the eastward flow characteristic of the upper layers reversed below 600 dbar.

The distribution of thermohaline properties at 10 dbar (Figure 6), evidence the effect of eddy-induced outcropping of the thermocline at the eddy centre. At this depth, the upper water column was >0.4°C cooler and >0.04 psu saltier at the eddy centre than in waters outside the eddy (Figure 6A,B). The 25.25 isopycnic surface showed a sloping from $\sim$28 m in the peripheral region to less than 8 m at the top of the SWODDY core, a rather density-homogeneous region (Figure 6C).

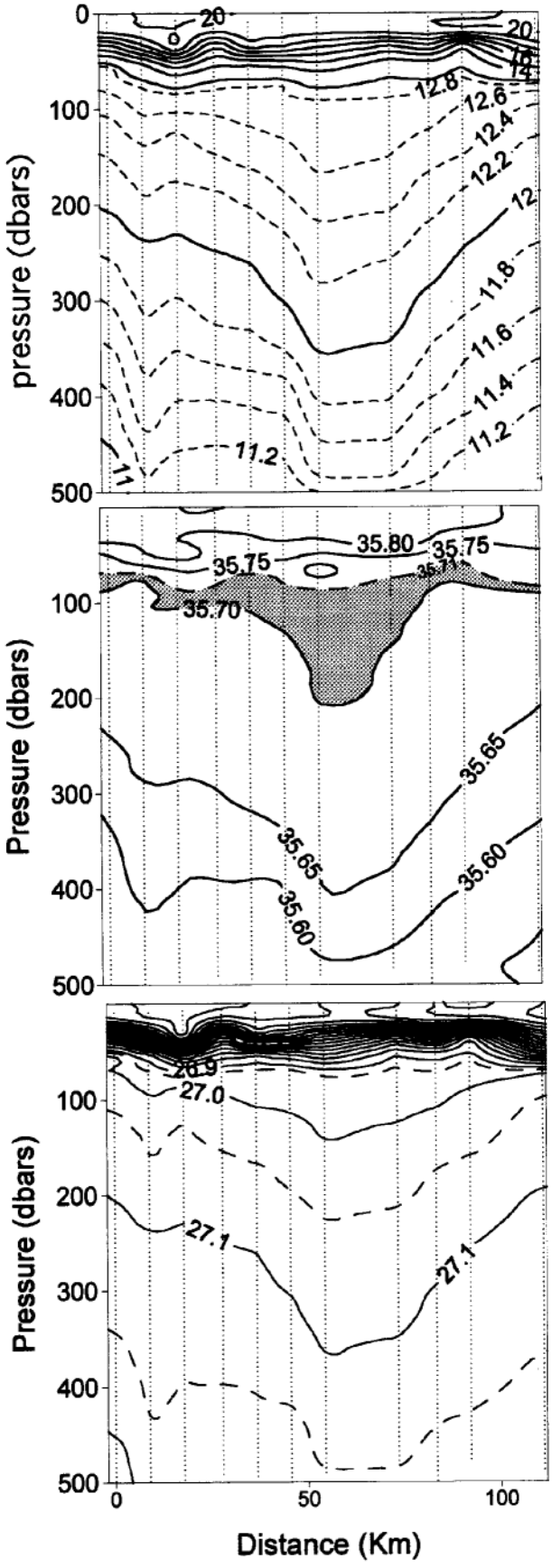

Figure 4. Latitudinal section (St. 31 to 60; see Figure 3) of temperature (°C), salinity and sigma-t through the slope water oceanic eddy AE6.

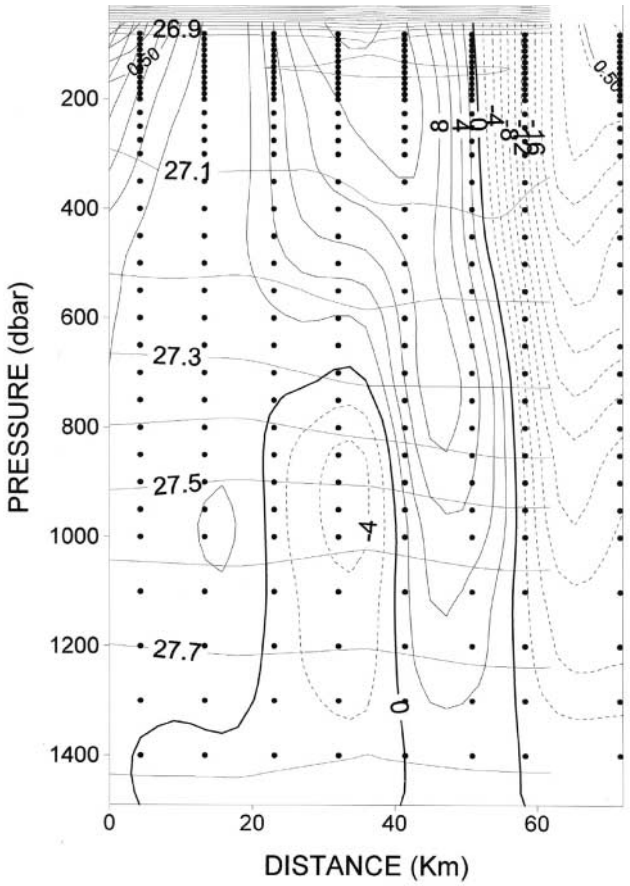

Figure 5. Geostrophic velocities (cm s^{-1}) across the slope water oceanic eddy AE6 (St. 31 to 49 see Figure 3). Sigma-t values are also overlapped. Dotted lines indicate negative (westward) velocities.

In this paper, two perpendicular sections of CTD stations, both of them converging at the eddy centre, were selected to describe the spatial distribution of chemical and biological variables (Figure 7). Sampling of the two sections was completed in three days. The thermohaline characteristics of the perpendicular sections (Figure 7) were similar to those described above (see Figure 4). Differences in the vertical location of isotherms and isohalines between both sections reflected the lack of synopticity caused by the sampling of 'biological' stations (St. 20 and 27 at the eddy centre and 23 and 31 outside the eddy) that lasted 24 h. As a consequence, the eddy centre (St. 20 and 27) was visited with a two days off-set. The warm and saline subsurface core of the eddy as well as the doming of the seasonal pycnocline was clearly manifested.

Nitrate and dissolved oxygen

The distribution of dissolved nitrate (Figure 8) closely followed the density structure of the upper 500 dbar of the water column. Nitrate was exhausted ($<0.5\,\mu$mol l^{-1}) in the upper mixed layer. The nitracline was located at 50–75 dbar, depending on the station. The vertical location of the nitracline was associated with that of the seasonal pycnocline (e.g. St. 20). At subsurface layers and for a given depth, nitrate concentration was lower at the core of the eddy than at outside waters. Ammonium

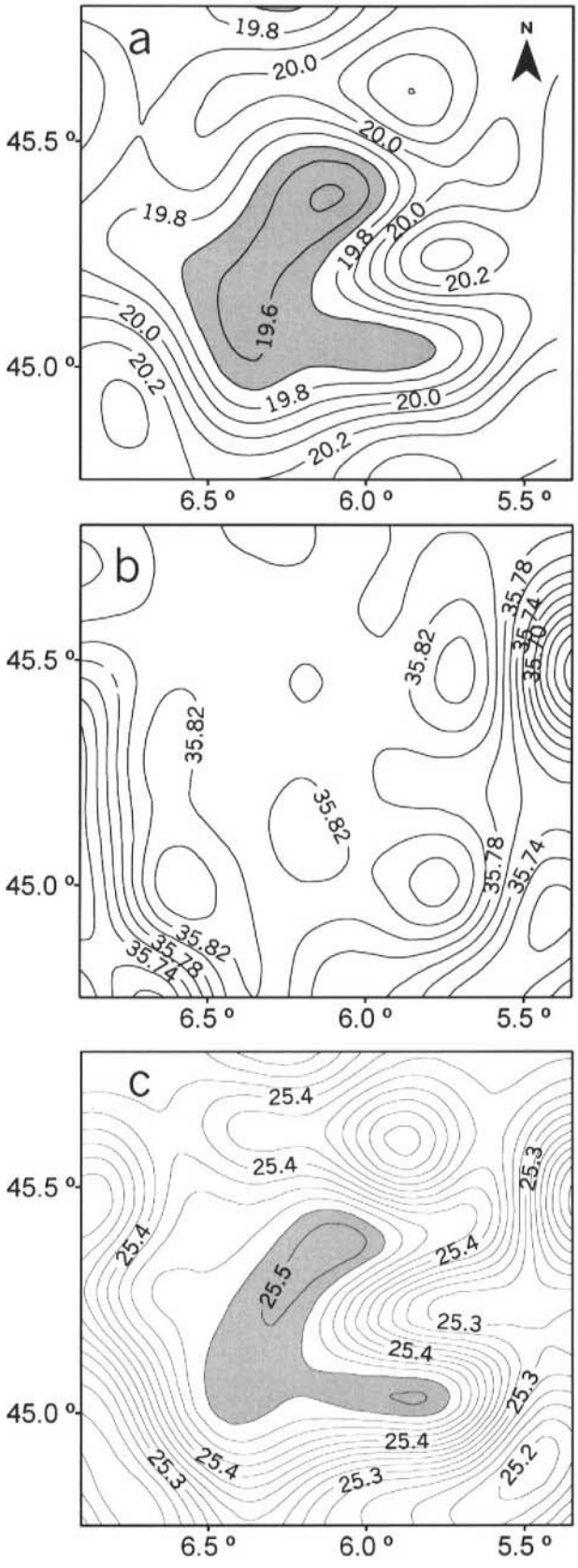

Figure 6. Horizontal distribution of: (A) temperature (°C); (B) salinity, and (C) sigma-t at the 10 m isobath.

concentrations were low in surface waters both inside and outside the eddy ($<0.2\,\mu$mol l^{-1}). Relatively higher dissolved oxygen concentrations were measured in the upper 100 dbar than below this depth. Maximum values

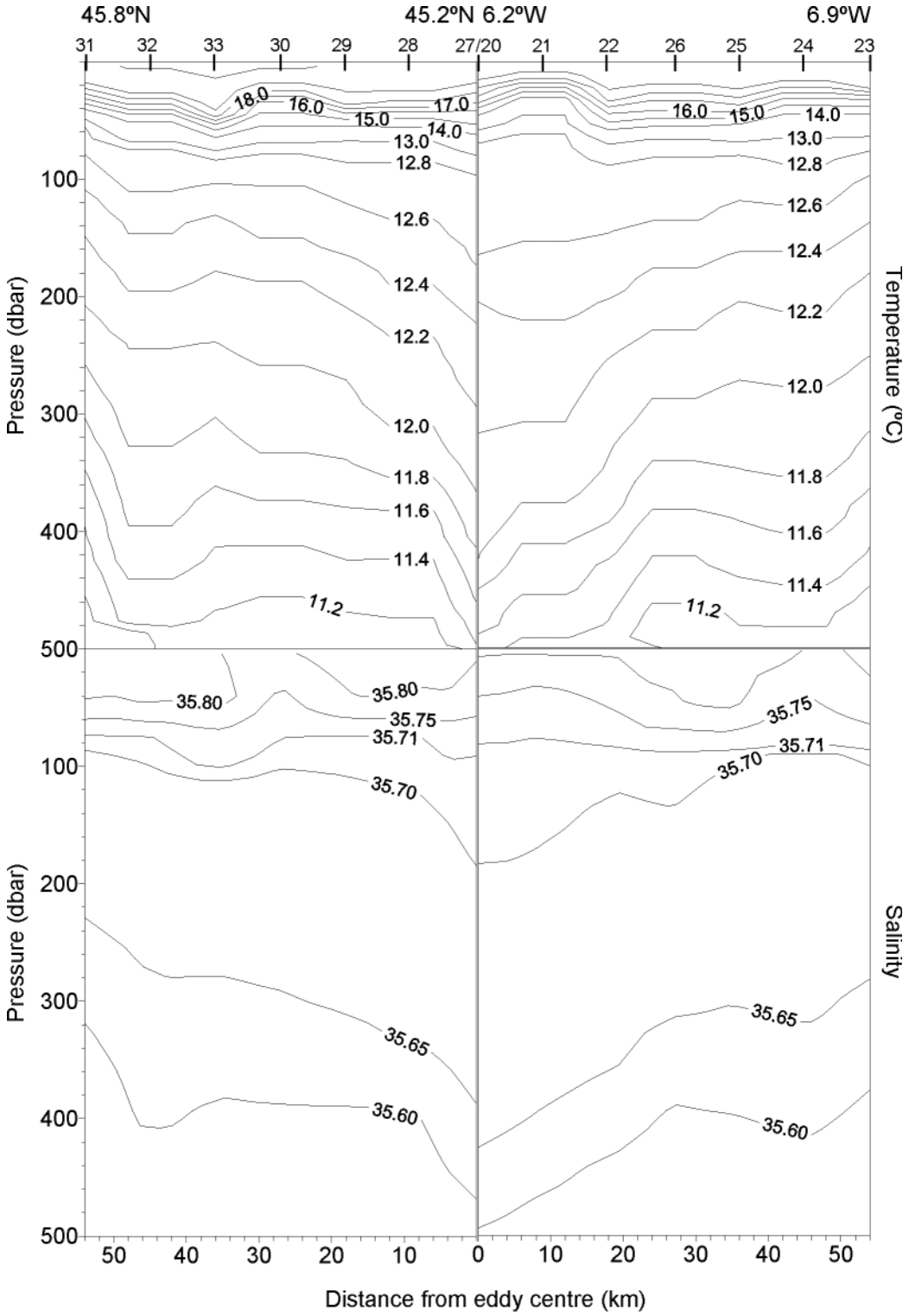

Figure 7. Vertical section (500 m) of temperature (°C) and salinity along the E–W, N–S intensive section (for the location of stations see Figure 3).

were associated with subsurface layers where a chlorophyll (chl) *a* maximum developed (see Figure 9). Relatively low oxygen concentration characterised the core of the eddy from 100 to 250 dbar.

Mesoscale spatial and short-scale temporal chlorophyll a *distribution*

The distribution of chl *a* in the upper 100 dbar of the perpendicular section together with the accompanying thermal field is represented in Figure 9. At St. 21, located at the eddy centre, doming of the thermocline is shown. Chl *a* concentrations in the upper 20 m of the water column were always lower than 0.05 mg m^{-3}. SeaWiFS chl *a* observations near the sampling time (7 August 1998; Garcia-Soto et al., 2002) did not show a significant chl *a* increase near the eddy centre though the satellite values were higher at the northern and eastern margins were the gradient of dynamic height (and associated geostrophic

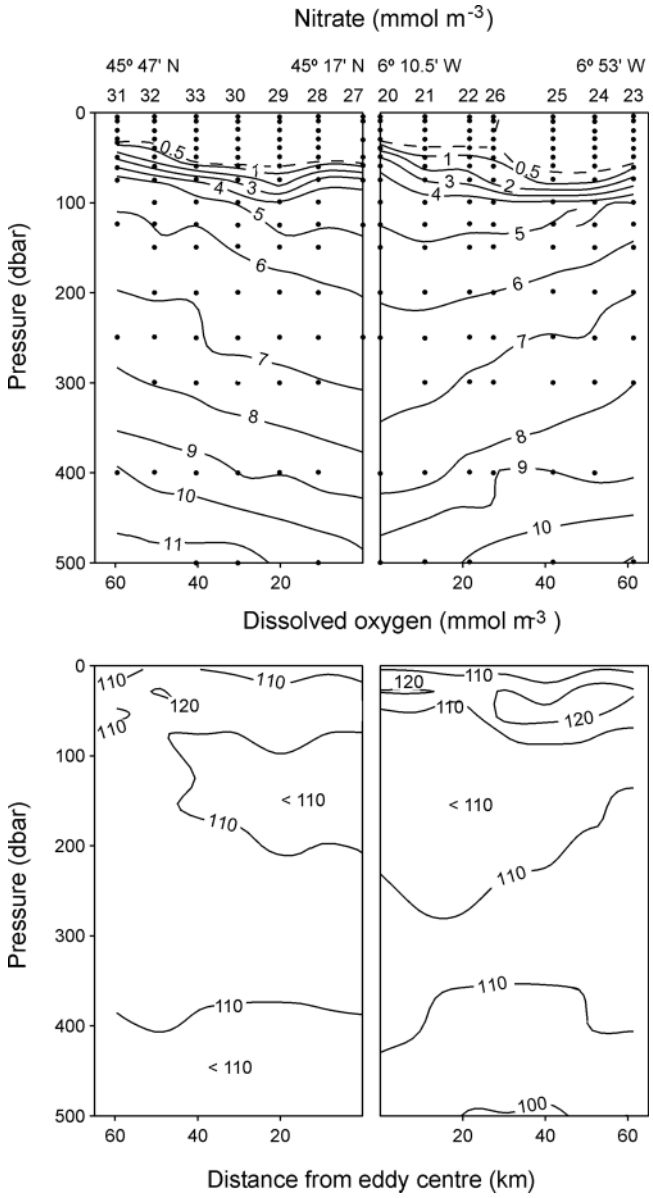

Figure 8. Vertical section (500 m) of dissolved inorganic nitrate and oxygen along the E–W, N–S intensive section (for the location of stations see Figure 3).

currents) was more intense. *In situ* data depicted a distinct subsurface chl *a* maximum (SCM) at all the stations, typically at 50–70 dbar. The vertical position of the SCM was shown, however, to be variable at the eddy centre. Whereas, it was located at 40 dbar at stations 20 and 21, it was measured at 70 m at station 27. The magnitude of the SCM at the eddy centre was always higher (0.4–0.6 mg m^{-3}) than at the rest of stations.

The drastic changes in the vertical location of the SCM at the eddy centre (30 dbar) appear to be related to the interaction between the seasonal pycnocline and the passage of short-period perturbations, internal waves, through the eddy region. The continuous deployment of CTD casts at the eddy centre (45.2°N 6.3°W) for 4 hours illustrate the large variability at short time scales in the thermal structure of the upper water column in the region (Figure 10). Vertical excursions of the isotherms of up to 20 m were measured over temporal scales of about 10 minutes. The subsurface chl *a* maximum, initially located at 50–55 dbar, displayed excursions of the same spatial extension and temporal period as those described for the isotherms. The spatial continuity of the SCM seemed to become disrupted when the amplitude of the perturbation was more intense, possibly as a result of shearing within the layers, although we cannot discard that this effect were the result of a contouring artefact. The magnitude of the SCM remained rather constant with values ranging from 0.4 to 0.7 mg m^{-3}, a range similar to that measured at CTD stations 20 and 27. The vertical displacements of isotherms and the SCM measured in this exercise were of the same magnitude to those observed at the two stations corresponding to the eddy centre (st. 20 and 27) sampled along the perpendicular sections (see Figure 9). Very similar results were obtained when the same sampling strategy was conducted in waters located outside anticyclonic eddy AE6 (44.7°N 5.8°W). In this case, however, the SCM was located 1020 dbar deeper.

Clear differences in photic-depth integrated chl *a* concentration were identified between the eddy centre, the eddy margin and waters outside the eddy (Figure 11). Maximum depth-integrated chl *a* concentrations, exceeding 25 mg chl *a* m^{-2}, were measured at stations 20 and 21, located at the eddy centre (see Figure 9). By contrast, minimum values were found at stations separated 20–30 km from the centre, i.e. in the region where maximum geostrophic velocities were calculated (see Figure 4). Hence, stations at the eddy centre displayed chl *a* concentrations up to 48% higher as compared to the surrounding waters. The contribution of $>10\,\mu$m phytoplankton cells was consistently higher inside the eddy ($>20\%$) as compared with the surrounding waters where typical values were $\sim 17\%$ (Table 4).

The same patterns of spatial variability detected in phytoplankton biomass were also manifested from the absorption characteristics of the suspended particulate matter (Table 2). The absorption coefficients of total particulate matter and chlorophyll-containing particles were higher, almost by a factor of 2, at the centre than outside the eddy, both at surface waters and at the depth of the 1% isolume. The relative contribution of non-photosynthetic particulate matter to total suspended particulate matter did not show noticeable spatial differences, accounting on average for $\sim 20\%$ of total absorption. Significant differences were neither found in the PAR vertical attenuation coefficient. However, the spectral extinction of photons by the eddy waters clearly differed from those not influenced by the mesoscale structure. The relationship between the attenuation coefficients at 440 and 660 nm displayed a two-fold increase inside the eddy (Table 2). This sharp change in the relative seawater absorption of blue and green light derived mainly from an important reduction of the absorption at 660 nm rather than from a marked enhancement of the corresponding absorption at 440 nm inside the eddy, and suggests the existence of distinct phytoplankton populations inside and outside the SWODDY.

Phytoplankton species distribution

The microscopic examination of the planktonic primary producers revealed that waters inside and outside the eddy also differed in terms of the relative dominance of

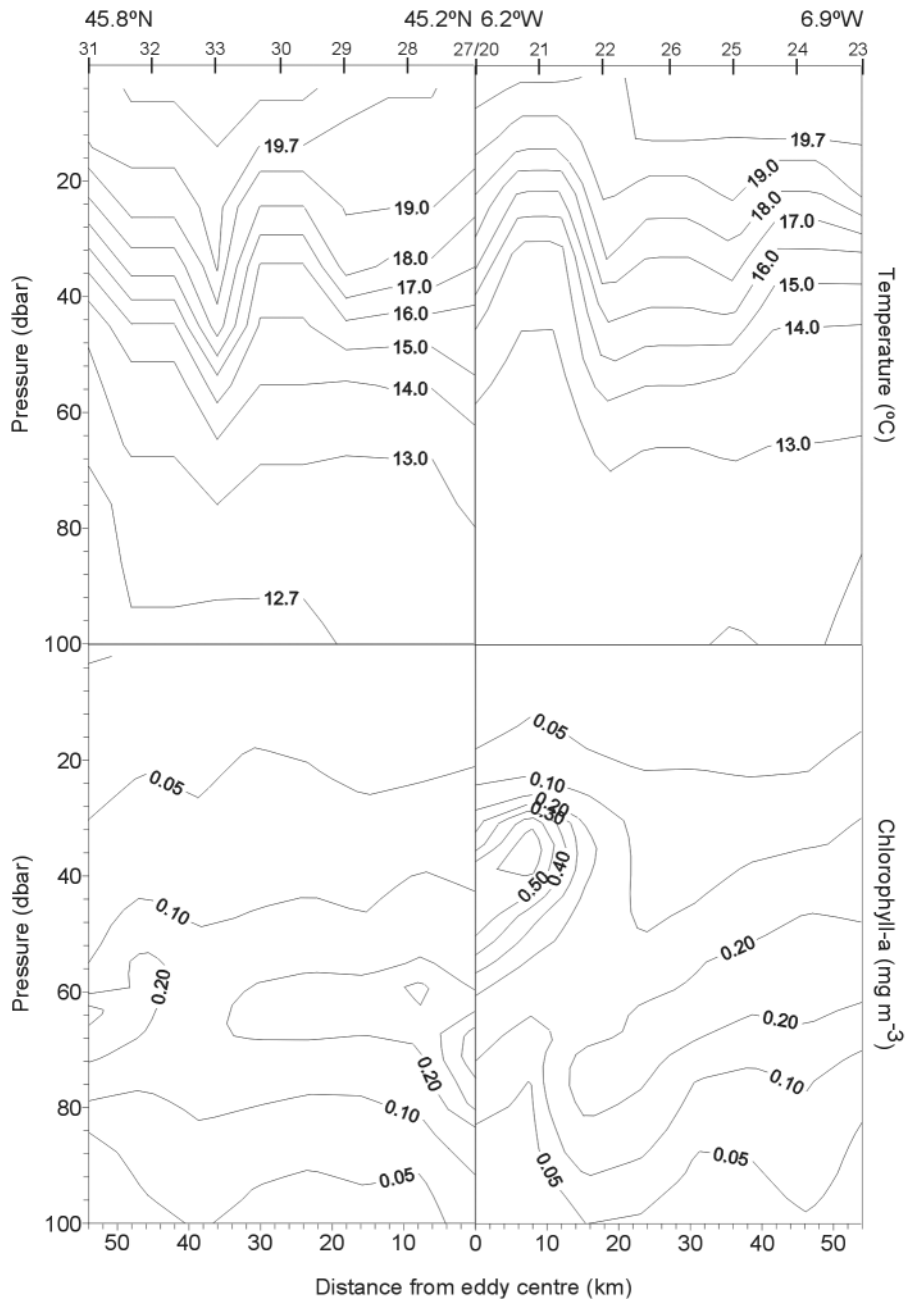

Figure 9. Vertical section (100 m) of temperature and chlorophyll *a* along the E–W, N–S intensive section (for the location of stations see Figure 3).

phytoplankton assemblages (Figure 12). Dinoflagellates, cryptophyceans and small unidentified flagellates ($<10\,\mu$m) were the most abundant phytoplankton groups. Their distribution was rather homogeneous across the eddy. Among dinophyceans, *Cachonina niei*, and small dinoflagellates ($<30\,\mu$m) dominated, with average number of cells exceeding 6 and 30 cells ml^{-1}, respectively. Representative species of this group were also *Ceratium lineatum*, *Gonyaulax polygramma*, *Triadinium polyedricum*, *Oxytoxum sphaeroideum*, *Prorocentrum micans* (with averaged abundances always <1 cell ml^{-1}) and several species of the genus *Gyrodinium* and *Gymnodinium*. By contrast, diatoms and chrysophyceans presented a distribution closely associated with the mesoscale structure (Figure 12). Diatoms were clearly concentrated in the central part of the eddy. Their abundances were remarkably higher in the subsurface layer below 40 dbar, approximately coinciding with the location of the SCM. Several species of the genus *Pseudo-nitzschia* were the most common diatoms, with mean values of >25 cells ml^{-1}. *Nitzschia longissima*, *Lioloma pacificum* and small centric and pennate diatoms were also present, but their abundances never exceeded 1 cell ml^{-1}. Chrysophyceans were represented especially by the silicoflagellates *Dictyocha fibula* and *D. speculum*, and the epibiontic flagellate *Solenicola setigera*.

The comparison of HPLC absolute and chlorophyll *a*-normalized pigment concentrations between stations 20 and 23, located at the eddy centre and outside the eddy respectively (Table 3), confirmed the results obtained from microscopic analysis. Thus, fucoxanthin, a pigment marker for diatoms and chrysophyceans, showed higher absolute and relative concentrations at the SCM inside the eddy.

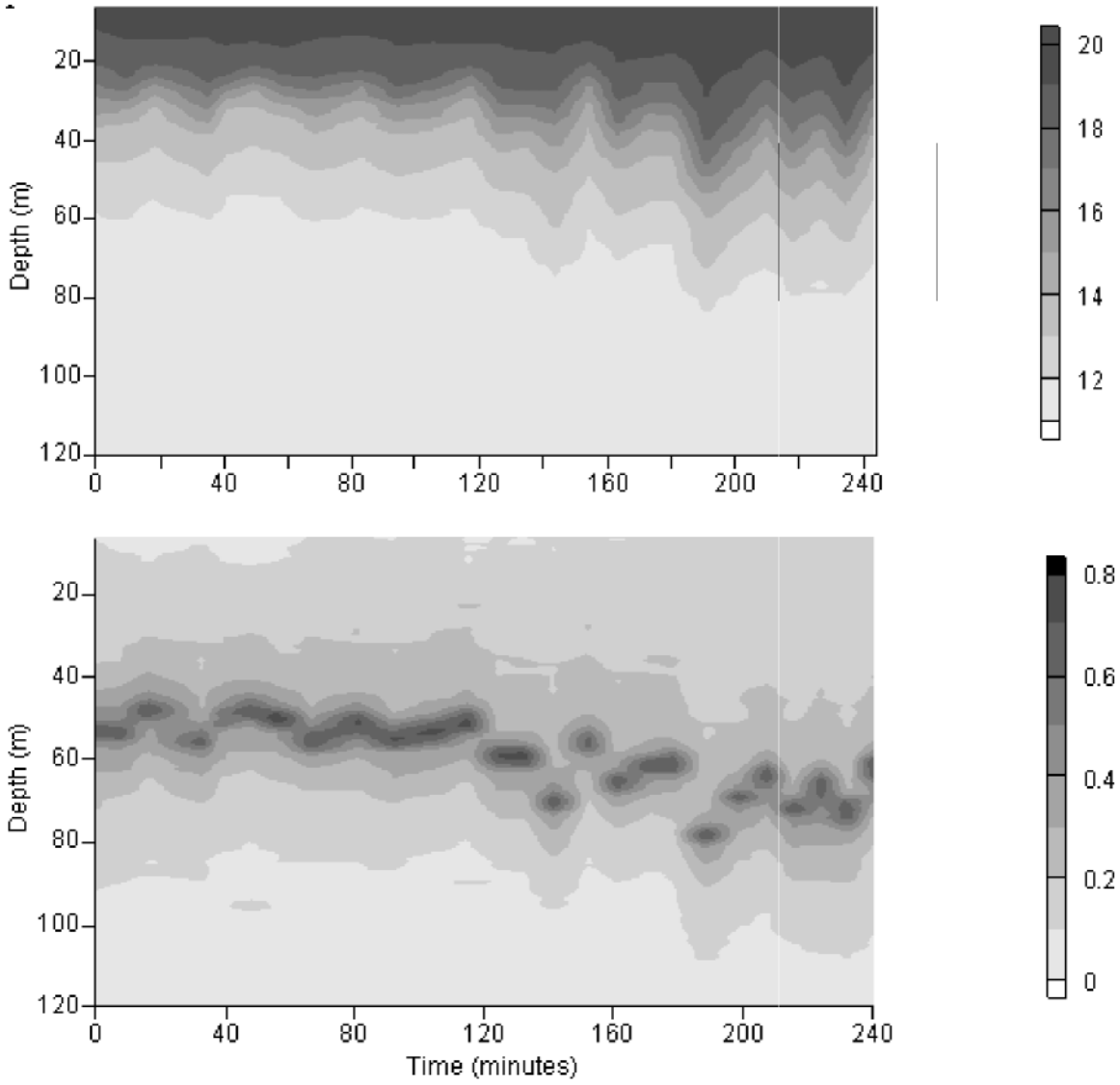

Figure 10. Short-term vertical distribution of: (A) temperature (°C), and (B) chlorophyll *a* concentration (mg m^{-3}) at the eddy centre (45°11.10′N 6°16.10′W).

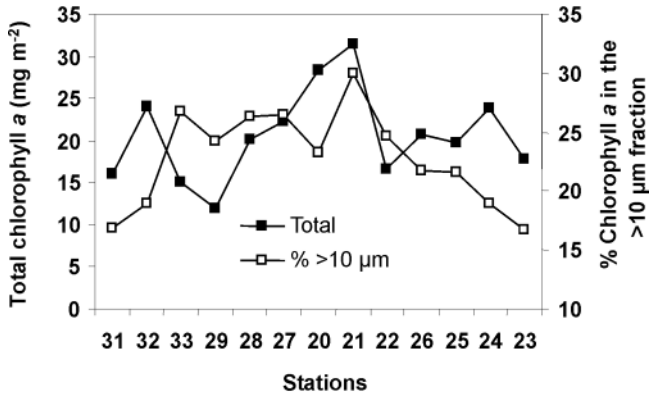

Figure 11. Spatial distribution of depth integrated chlorophyll *a* (100 m) and the relative contribution of $>10\,\mu$m phytoplankton cells to total chlorophyll *a* along the E–W, N–S intensive section.

Nevertheless, HPLC analysis of photosynthetic pigments also allowed us to gain additional insight into the composition of the phytoplankton population that was not perceivable by microscopic analysis of seawater samples. Cyanobacteria were shown to be considerably more abundant outside the eddy, both at surface and at the SCM, as revealed by the differential distribution of the carotenoid zeaxanthin. A thorough description of phytoplankton pigments inside and outside the eddy is available in Rodriguez et al. (2003). Briefly, a similar distribution pattern was observed at the SCM for chl *b* and peridinin, markers of chlorophycean and specific dinoflagellate assemblages respectively, although in the latter case the differences only apply to its relative importance with respect to the total biomass of photosynthetic organisms. Pigment markers characteristic of the class prymnesiophyceae, the carotenoid 19′ hexanoyloxyfucoxanthin and non-polar chl c2 presented higher concentrations at the eddy centre than outside the eddy. However, their relative contribution, i.e. their pigment/chl *a* ratios, were either higher inside the eddy (non-polar chl c_2) or outside the eddy in the case of the above mentioned carotenoid.

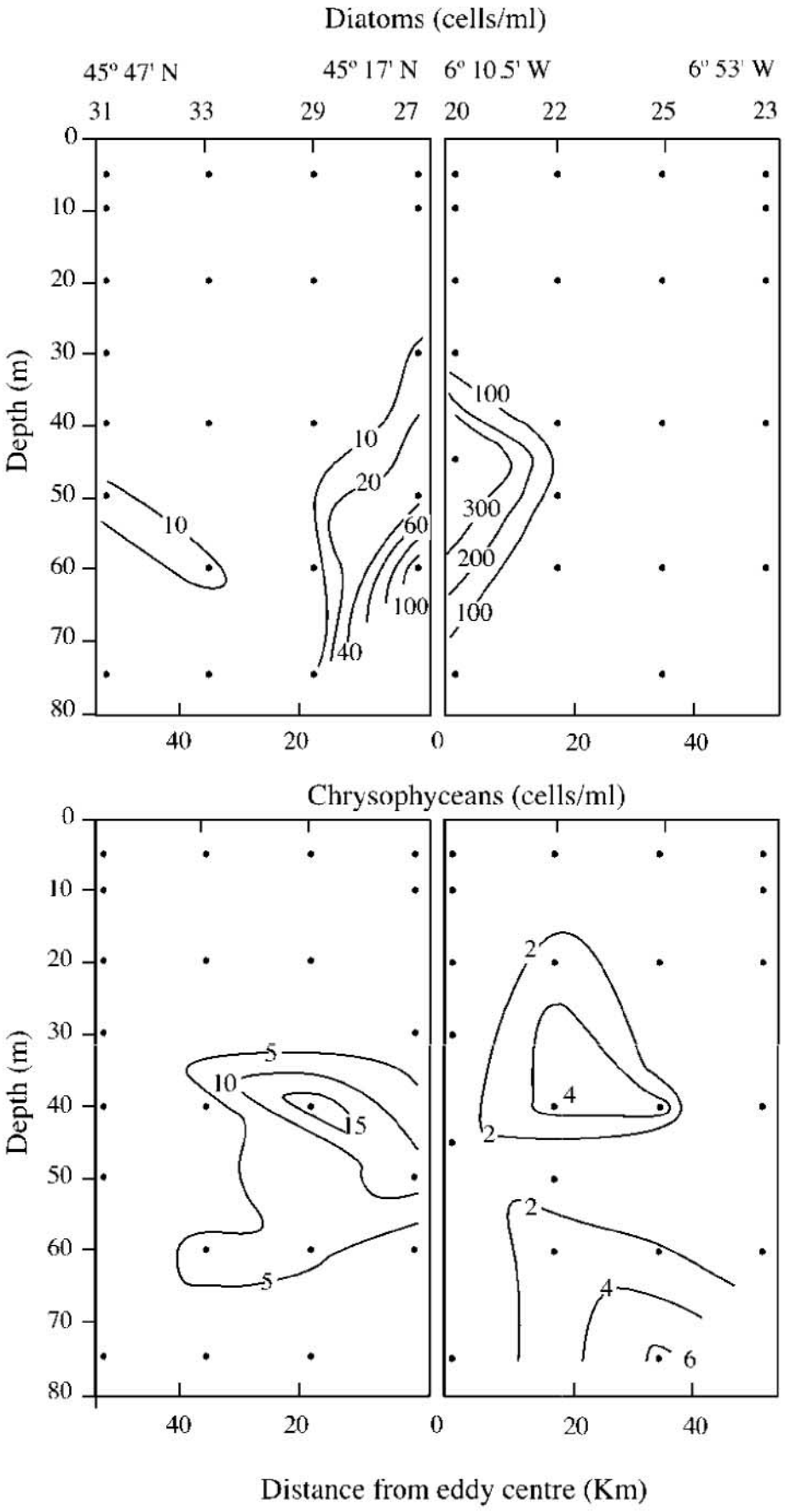

Figure 12. Vertical distribution of the abundance (cell ml^{-1}) of diatoms and chrysophyceans along the E–W, N–S intensive section.

Table 3. *Pigment concentrations and pigment ratios at surface and at the subsurface chlorophyll maximum (SCM) of station 20 (eddy centre) and 23 (outside eddy) determined by HPLC analysis. SCM was located at 45 and 60 dbar at stations 20 and 23, respectively.*

Pigment	Eddy centre (St. 20) $\mu g\,m^{-3}$	Outside Eddy (St. 23) $\mu g\,m^{-3}$	Eddy centre (St 20) pigment/chl *a*	Outside Eddy (St. 23) pigment/chl *a*
Surface				
Chlorophyll *a*	17.5	22.6		
Non-polar chlorophyll c_2 '*Chrysochromulina* type'	3.8	3.6	0.217	0.159
19′ Hexanoyloxyfucoxanthin	2.6	8.3	0.149	0.367
Zeaxanthin	2.1	9.1	0.120	0.402
SCM				
Chlorophyll *a*	745.4	176.4		
Chlorophyll *b*	100.3	112.6	0.135	0.638
Non-polar chlorophyll c_2 '*Chrysochromulina* type'	15.6	3.1	0.021	0.018
Non-polar chlorophyll c_2 '*Emiliania huxleyi* type'	22.9	3.1	0.031	0.018
19′ Butanoyloxyfucoxanthin	34.2	16.5	0.046	0.094
Fucoxanthin	61.1	24.3	0.082	0.138
19′ Hexanoyloxyfucoxanthin	275.6	80.4	0.370	0.456
Peridinin	13.8	13.8	0.019	0.078
Zeaxanthin	25.1	14.1	0.034	0.080

Table 4. *Depth-integrated phytoplankton biomass, primary production, new production and net community production rates and estimated diffusive nitrate fluxes at stations located inside (St. 20 and 27) and outside (St. 23 and 31) the slope water oceanic eddy (AE6).* f *ratio computed from euphotic zone-integrated uptake rates.*

	St. 20 Eddy centre	St. 27 Eddy centre	St. 23 Outside eddy	St. 31 Outside eddy
Depth integrated (100 m) chl *a* (mg chl *a* m^{-2})	22.2	28.4	16	17.8
Relative contribution of >10 m chl *a* (%) to total chl *a*	27	23	17	17
Depth integrated (100 m) biomass of autotrophic flagellates (mg C m^{-2})	105.1		77	
Photic zone (1% Io) integrated total primary production rates (mg C $m^{-2}\,d^{-1}$)	247	357	169	340
Relative contribution of < 2 m primary producers (%) to total primary production rate	24	38	38	46
Relative contribution of 2–10 m primary producers (%) to total primary production rate	28	24	18	15
Relative contribution of > 10 m primary producers (%) to total primary production rate	48	37	45	39
Photic zone (1% Io) integrated net community production (g O_2 $m^{-2}\,d^{-1}$)	−2.7	0.2	4.4	0.3
Eddy diffusion coefficients (Kz; $cm^2\,s^{-2}$)	$1.8\ 10^{-5}$	$1.4\ 10^{-5}$	$7.8\ 10^{-6}$	$7.8\ 10^{-6}$
Estimated diffusive nitrate fluxes (mmol N $m^{-2}\,d^{-1}$)	0.075	0.039	0.080	0.023
Photic zone (1% Io) integrated new production (mmol N $m^{-2}\,d^{-1}$)	0.41	0.77		0.91
Photic zone (1% Io) *f* ratio	0.1	0.14		0.29

Primary production, new production and net community production

On average, the photic-depth integrated rate of carbon incorporation by phytoplankton was slightly higher at stations located at the eddy centre (302 mg C $m^{-2}\,d^{-1}$) than outside the eddy (254 mg C $m^{-2}\,d^{-1}$) (Table 4). A marked subsurface primary production maximum, located between 30 and 40 dbar, was observed at most of the stations. About 40% of the total amount of carbon incorporated by phytoplankton flowed through the >10 μm size fraction, either inside or outside the eddy. New production was low in all stations, both inside and outside the eddy, and ammonium was the main source of inorganic nitrogen for primary production, as *f*-ratio values were always <0.5. The large within-site variability measured for all these variables implied that the differences encountered in *f*-ratio between waters inside and outside the eddy were not statistically significant even when all the stations where new production experiments were conducted were considered ($P>0.05$, N=11). The same applies to the rate of net community production which, on average, was negative at the eddy centre and positive outside. However, the analysis of individual stations 20 and 27 indicated that within the eddy the balance between oxygen production and respiration could be either positive or negative.

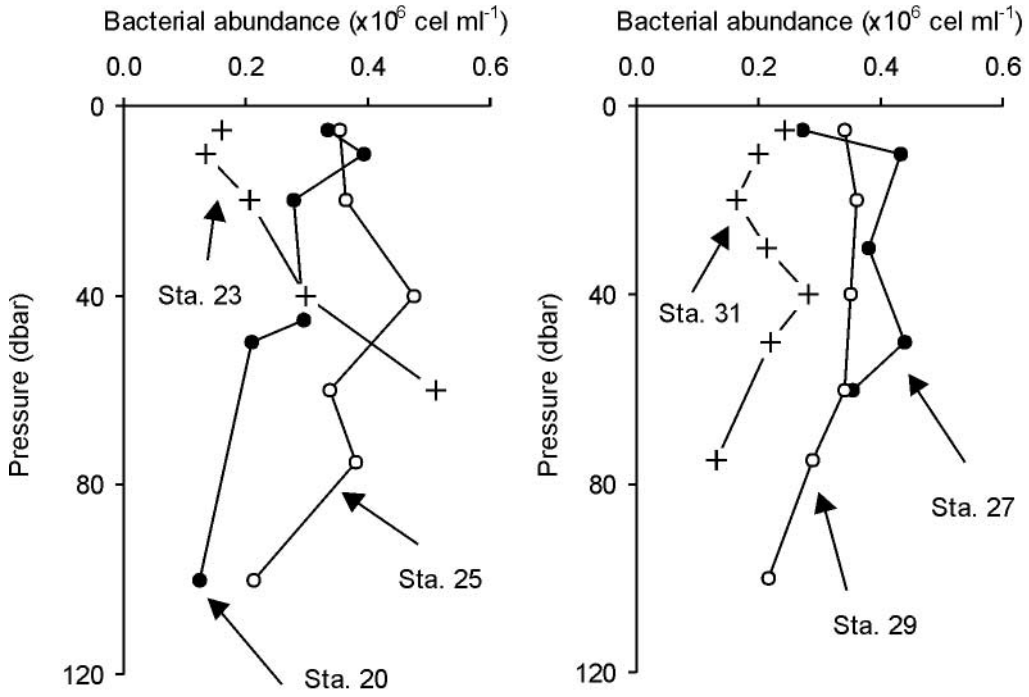

Figure 13. Vertical profiles of bacterial abundance ($\times 10^6$ cell ml^{-1}) at stations located at the eddy centre (20, 27), inside the eddy (25, 29) and outside the eddy (23, 31).

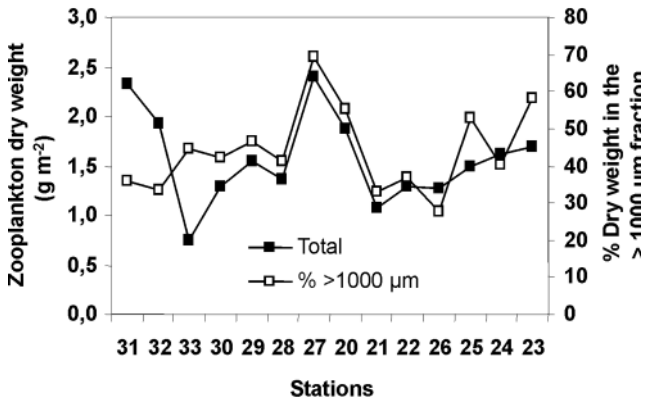

Figure 14. Spatial distribution of depth integrated (200 m) mesozooplankton (>200 um) biomass (dry weight) along the E–W, N–S intensive section.

Bacterial abundance

The abundance of bacterial cells at selected stations of the perpendicular CTD section typically ranged from 1×10^5 to 5×10^5 cells ml^{-1} (Figure 13). In general, bacterial abundance was higher at stations located inside (St. 20, 25, 27 and 29) than outside (St. 23 and 31) the eddy. The depth distribution of bacterial numbers did not display a consistent distribution pattern. Thus, bacterial abundance decreased with depth at most of the stations located inside the eddy, whereas in the surrounding waters, they were either more abundant at depth (St. 23) or showed a considerable degree of vertical variability (St. 31). On average, depth integrated bacterial biomass was higher at stations located at the eddy centre (370 mg C m^{-2}) than outside the eddy (203 mg C m^{-2}).

Zooplankton biomass and composition

The distribution of >200 μm mesozooplankton biomass along the perpendicular CTD section largely resembled that of depth-integrated chl *a* (Figure 14). Maximum dry weight values of >1.5 g m^{-2} were measured at the central stations of the SWODDY and also at stations located at the northernmost end of the transect. The lowest dry weight values (<1 g m^{-2}) were found 20–30 km away from the eddy centre, coinciding with the region where the minimum chl *a* concentrations were observed. Mesozooplankton organisms were not only more important in terms of biomass at the eddy centre but they were also larger. At the eddy centre, animals larger than 1 mm accounted for more than 50% of the total mesozooplankton dry weight. Their numbers decreased down to 30–40% at the rest of the sampled stations, except at st. 25 and 23 where they exceeded 40%.

In spite of the higher zooplankton dry weight detected at the eddy centre, their abundance was significantly higher outside the eddy, where more than 7×10^4 ind m^{-2} were found, than inside ($\sim3.5\times10^4$ ind m^{-2}) (Table 5). This mismatch can be explained from the differences in community size structure mentioned above and is consistent with the higher proportion of juvenile copepods and euphausiids registered at stations located outside the eddy. This pattern was not observed at station 23. At all the stations, copepods represented more than 87% of the total number of mesozooplankton individuals.

Sharp changes in mesozooplankton community species composition resulted from the presence of the SWODDY (Table 5). Typical coastal-neritic (*Acartia clausi*) or shelf/shelf-break copepod species (*Euchaeta hebes*) appeared exclusively inside the eddy. By contrast, oceanic epipelagic and mesopelagic species such as *Pleuromamma abdominalis*,

Heterorhabdus norvegicus, *Calocalanus styliremis* and *Disconchoecia elegans* were absent from the interior of the mesoscale structure. Appendicularians were found almost exclusively outside the eddy. It is worth noting the differential distribution of the chaetognaths *Sagitta serratodentata* and *Sagitta friderici*. Thus, whereas *S. serratodentata*, a characteristic oceanic species inhabited only waters outside the eddy, whereas the neritic species *S. friderici*, appeared only inside the eddy.

DISCUSSION

The results presented in this paper demonstrate that Slope Water Oceanic eDDIES (SWODDIES), a recurrent mesoscale feature in the Southern Bay of Biscay (Pingree & Le Cann, 1992a; García Soto et al. 2002), significantly modify the ecological characteristics of the planktonic communities of the region during the period of vertical thermal stratification.

Infra-red satellite images evidence that warm slope water flows along the western and northern Spanish coast during winter. On some locations this slope water is injected into the deep regions of the Bay of Biscay thereby generating slope water anticyclonic eddies (Pingree & Le Cann, 1992a). Unfortunately, for the investigation presented here it was not possible to have a sequence of cloud-free AVHRR images linking clearly AE6 to an slope water origin. We note however that the winter of 1997/1998 preceeding the cruise was a year of exceptional poleward flow along northern Spain and that at least two winter swoddies (21/22 January AVHRR observations) were shed to the ocean from near Cape Ferret canyon (F98) and Cape Ortegal (O98) (Garcia-Soto et al., 2002).

The anticyclonic eddy AE6 was a typical slope water anticyclonic oceanic eddy. The thermohaline properties of AE6, closely resembled those of SWODDIES previously studied in the same region such as F90a (Pingree & Le Cann, 1992a) and X91 (Pingree & Le Cann, 1992b). All these eddies showed a characteristic homogeneous core of water at the ring centre which extended from 65–70 to >200 dbar. The core of AE6 was slightly colder, less saline and denser than F90a. By contrast, as compared with X91, AE6 was warmer (11.5–12°C in X91). The maximum geostrophic velocity of AE6, observed 30 km from the eddy centre was slightly lower than the 30 cm s^{-1} calculated for F90a. Differences in the thermohaline properties of the eddy cores are likely to reflect interannual thermal changes in the slope water, which typically vary within a range of ±2°C (see Figure 3 in Pingree & Le Cann, 1992b). An alternative, but not exclusive, explanation for the observed differences could be a northern or deeper source of the slope water originating AE6 as compared with F90a. The properties of the core have been shown to vary little over shorter (20 days) time scales (Pingree & Le Cann, 1992a).

The results shown in this investigation demonstrate that anticyclonic eddies do not always give rise to downward depression of isopycnals and associated motion of nutrient-depleted water within the photic layer. The vertical thermal structure of the SWODDY investigated in this study (Figure 6) is similar to the anticyclonic eddy ACl described in the Sargasso Sea (see figure 2 in McGillicudy et al., 1999). ACl was composed of a thick lens of 18°C water that depressed the main thermocline while raising the seasonal thermocline, resulting in a shoaling and increase in magnitude of the deep chlorophyll maximum. In this case as in the SWODDY AE6, depression of the main thermocline has a larger contribution to the geostrophic shear than uplifting of the seasonal pycnocline, originating the anticyclonic circulation characteristic of this feature. These eddies also have a similar origin, as it has been hypothesized that ACl was formed by convective mixing during the previous winter near a seamount chain (McGillicudy et al., 1999).

Depth-integrated chl *a* concentrations were significantly higher inside than outside the eddy (Figure 11). Pingree & Le Cann (1992a) already postulated that the doming of the pycnocline characteristic of SWODDIES, which results from a 'partial response towards hydrostatic equilibrium of the slope core within the surrounding ocean', might have implications for phytoplankton productivity. Continuous chl *a* sections conducted across the slope water eddy F90a using Seasoar, show comparable results to those shown here (see Figures 15 and 16 of García-Soto et al., 2002). We are aware, however, that the submesoscale structure detected inside Swoddy AE6 (Sánchez and Gil, in press) could potentially affect the comparison between waters inside and outside the eddy. The description of higher chl *a* levels at the core of anticyclonic eddies have been previously reported (e.g. Tranter et al., 1980; Jeffrey & Hallegraeff, 1980, Krom et al., 1992), although in these cases the build up of phytoplankton biomass was induced by deep winter convective mixing of the eddy cores. Modelling studies of the upper layers of the ocean revealed that mesoscale eddy activity, through the upward displacements of the pycnocline, has a two way effect on biological production: a) an upward flux of new nutrients intto the photic layer and b) enhanced PAR irradiance levels, thereby enhancing primary production rates (Smith et al., 1996).

Tilting of isopycnal surfaces favours vertical transport of nutrient-rich isopycnal surfaces into the euphotic zone and, as a consequence, a close relationship has been reported between doming of the pycnocline and nitracline, maximum values of vertical velocity and enhanced chl *a* levels in mesoscale structures (e.g. Pinot et al. 1995). A relaxation in the constraint of nutrient limitation could thus lead to a stimulation of primary production and a corresponding increase in phytoplankton biomass. With the aim of estimating the fraction of new production accounted for by nitrate entering the photic layer by eddy diffusion at the eddy centre, we estimated the flux of nitrate across the deep chlorophyll maximum from the product of the estimated diffusion coefficients (Kz) and the gradients of nitrate concentration across the deep chlorophyll maximum (0.033–0.124 mmol m^{-1}). The estimated fluxes, ranged from 0.039 to 0.075 mmol $m^{-2}d^{-1}$ (Table 4). Daily new production rates at the eddy centre, estimated from the measured nitrate uptake rates (Table 4), ranged from 0.41 to 0.77 mmol N m^{-2} d^{-1}. Thus, the resulting diffusive fluxes of nitrogen accounted for ~5–18% of the nitrogen required to sustain the measured rate of new production. We are aware that the way daily new production rates were calculated in this study (assuming a constant 24 h N incorporation rate) is likely to overestimate the actual value of this rate. Nevertheless, an

Table 5. *Abundance (ind m^{-2}) of mesozooplankton species at stations located inside (St. 20 and 27) and outside (St. 23 and 31) the slope water oceanic eddy (AE6).*

	St. 20 Eddy centre	St. 27 Eddy centre	St. 23 Outside eddy	St. 31 Outside eddy
Total individuals	35261	37744	70633	195792
Total copepods	34242	35826	66471	171362
% copepods	97	95	94	88
% juvenile copepods*	9	5	16	13
% juvenile euphausiids*	38	3	76	63
No copepod species	36	33	25	34
Species dominant outside the eddy				
Clausocalanus pergens	15979	14817	22974	52577
Clausocalanus lividus	40	207	5873	4122
Centropages typicus	8	16	748	3891
Mesocalanus tenuicornis	374	48	684	4838
Appendicullariaceans	0	32	1854	11189
Species exclusive of waters outside the eddy				
Disconchoecia elegans	0	0	0	796
Heterorhabdus norvegicus	0	0	0	294
Calocalanus styliremis	0	0	525	2730
Pleuromamma abdominalis	0	0	16	16
Sagitta serratodentata	0	0	310	1058
Species dominant inside the eddy				
Heterorhabdus papilliger	40	72	8	0
Scolecithricella minor	1003	175	8	0
Species exclusive of the eddy				
Orthoconchoecia haddoni	80	64	0	0
Acartia clausi	175	0	0	0
Euchaeta hebes	477	0	0	0
Vettoria granulosa	119	8	0	0
Sagitta friderici	0	32	0	0

*, Percentage relative to the total abundance of copepods and euphausiids, respectively.

independent estimate of new production, based on the measured radiocarbon incorporation by phytoplankton, and assuming a C to N molar ratio equivalent to the Redfield value (6.6; Redfield et al., 1963) and a *f*-ratio typical of an oligotrophic oceanic region between 0.1 and 0.2 (Dugdale & Goering, 1967, Sahlsten, 1987), yielded rates ranging from 0.3 to 0.9 mmol N m^{-2} d^{-1} which were close to our direct estimates using nitrate uptake. Moreover, even assuming that nitrogen incorporation exclusively occurs during the light period, the estimated diffusive fluxes of nitrogen would represent less than 40% of the nitrogen required for new production. The results of these calculations suggest that diffusion appear to be of limited importance for the upward supply of nitrate to the photic layer both outside and inside the eddy and that other processes are likely to play a relevant role in the sustainability of new production in the Southern Bay of Biscay in summer. Calculations of vertical diffusive flux of nutrients in the mesoscale eddy field of the Sargasso Sea (Siegel et al., 1999) also showed that diapycnal diffusion was not a significant process transporting nutrients into the euphotic zone. Eddy diffusive mixing along sloping isopycnals is another mechanism that can transport nutrients into the upper productive layer (e.g. Jenkins, 1988), but this mechanism also appears to be of reduced relevance compared with eddy pumping (Siegel et al., 1999).

Although our results show that internal wave activity was of similar magnitude inside and outside the eddy, their effect on primary production is likely to be more conspicuous at the eddy centre where phytoplankton populations inhabiting the SCM are subjected to higher irradiance levels due to the in general shallower location of the thermocline. On average, the SCM was located 10 m shallower at the eddy centre (50 m) than outside the eddy. Assuming a vertical displacement of the averaged vertical location of the SCM of $\pm$7.5 m due to internal wave oscillations (see Figure 10), and using an average K_d of 0.0705 m^{-1} (Table 2), the irradiance reaching the SCM would range from 17 to 50 μmol m^{-2} s^{-1} at the eddy centre and from 9 to 25 μmol m^{-2} s^{-1} outside the eddy, representing 1.7–5% and 1.5–2.5% of surface irradiance, respectively. Hence, the irradiance at the SCM is approximately a two-fold factor higher inside than outside the eddy centre. The transient relatively high irradiance levels experienced by primary producers at the SCM inside the eddy is likely to explain the enhanced levels of phytoplankton biomass detected at the centre of SWODDY AE6 as compared with surrounding waters. Although this enhanced irradiance level does not necessarily translate into a proportional increase in phytoplankton carbon assimilation, it is possible that given the low irradiance levels characteristic of the SCM, the magnitude of primary production rates at the eddy centre were

significantly higher than those measured at surrounding waters. Although this result agrees with the rates of depth integrated primary production measured at selected stations during the cruise (see Table 4), the differences in the temporal scales associated with radiocarbon incorporation experiments ($\sim$6 h) and to internal waves (10–15 minutes) imposes serious constraints on our phytoplankton production estimates in such a highly variable environment.

Enhanced plankton biomass can also result from the concentration of particles by the flow field. Theoretical analysis has shown that non-motile particles can be trapped in certain areas within the eddy core (Flierl, 1977). If these mechanisms were of relevance in SWODDY AE6, an increase in the contribution of detrital material at the eddy centre would be expected, as reported by Nelson et al. (1985). However, we did not find any significant differences in the ratio between the absorption coefficients of chlorophyll-containing particles and total suspended particulate matter at stations located at the eddy centre or outside the eddy (Table 2). Not every species of primary producers responded in a similar way to the new environmental conditions set up by the eddy dynamics. The phytoplankton assemblages of the central region of the SWODDY were dominated by diatoms and chrysophyceans (Figure 12 and Table 3), thereby increasing the contribution of large cells ($>10\,\mu$m) to total phytoplankton chlorophyll (Figure 12). Similarly, Nelson et al. (1985) found a higher contribution of larger phytoplankton cells at the ring centre of a Gulf Stream warm core ring, a feature that generally results from the dominance of diatom populations (Jeffrey & Hallegraeff, 1980; Nelson et al. 1985; Gould & Fryxell, 1988). Recently, Rodríguez et al. (2001) have shown the existence of a direct empirical relationship between the relative proportion of large cells and the magnitude of the velocity of seawater in a frontal system in the range $\pm 5\,\mathrm{m\,d^{-1}}$. In this regard, based upon the observed vertical displacement of isopycnal surfaces with time, Joyce et al. (1984) estimated mean upward vertical velocities of 0.5 to $1.5\,\mathrm{m\,d^{-1}}$ at the centre of the warm core ring 82-B, values that lie within the range mentioned above ($\pm 5\,\mathrm{m\,d^{-1}}$). The higher biomass of larger primary producers observed in this study at the eddy centre (Figure 11) directly propagated through the food web favouring enhanced growth rates of large-sized mesozooplankton species (Figure 14).

SWODDIES are able to transport their core properties over long distances (>100 km) through the ocean (Pingree, 1984). Living particles are among the properties being transported by these eddies as the characteristic short response time allows planktonic organisms to maintain themselves within mesoscale features by their increased net population growth rates that work against diffusive processes (Angel & Fasham, 1983). This study clearly shows that phytoplankton and mesozooplankton populations not only exhibited higher biomass and a different size structure inside anticyclonic eddy AE6, but their taxonomic composition was different as compared with the surrounding waters. The exclusive presence of the silicoflagellates *Dyctyocha fibula* and *D. speculum* inside the eddy, both species characteristic of the autumn–winter period in the adjacent Central Cantabrian Sea (Fernández & Bode, 1994), when the poleward slope current develops, reflects the biological characteristics of the water body which initially originated SWODDY AE6. In addition, the HPLC pigment signature of samples from the eddy centre and those collected from the core of the poleward slope current on October 1999, was demonstrative of a high degree of similarity of phytoplankton species composition between these two hidrodynamic features (see also Rodríguez et al., 2003).

Nevertheless, the most distinct distributional pattern observed in this investigation was found for diverse species of mesozooplankton (Table 5). The presence of typical coastal-neritic or shelf/shelf-break copepod and chaetognath species exclusively inside the eddy and the occurrence of oceanic copepods and appendicularians only at stations outside the anticyclonic AE6, reinforce the role of these mesoscale features in the retention of typically coastal biological properties in open ocean waters. Our results, agree with previous findings in Kuroshio warm core-eddies showing enhanced zooplankton abundance and presence of coastal-neritic copepods (eg. *Acartia clausi*) and indicators of coastal waters such as cladocerans trapped by this structures in open ocean waters (Yamamoto & Nishizawa, 1986).

The sharp modification of the planktonic community composition, biomass and associated size-structure caused by the insulation of water parcels from coastal origin are likely to exert a profound effect upon the upper trophic levels of the pelagic ecosystem. In this regard, Sánchez & Gil (2000) reported an inverse relationship between the intensity of the eastward shelf-break poleward flow during October and hake recruitment indices due to offshore transport of larvae and pre-recruits, a mechanism that would be related to the generation of SWODDIES which could retain and export hake recruits far from the recruitment areas (Sánchez & Gil, 2000). The interaction of Slope Water Antyciclonic Eddies with larval fish transport mechanisms could, therefore, result in fluctuations in recruitment.

On a larger oceanic scale, oceanic SWODDIES, as the one presented in this study but observed before the establishment of the seasonal thermocline, have been shown to be characterized by lower chlorophyll *a* concentrations with respect to surrounding cyclones, probably as a result of the deeper mixed layer depth of these anticyclonic structures (see Figure 14A in García-Soto et al., 2002). Future ecological investigations of Slope Water Oceanic eDDIES might examine the trophic aspects of these relevant mesoscale eddy structures at the beginning of the productive season and during the spawning and recruitment of commercial fishes.

We wish to thank the captain and crew of RV 'Professor Shtokman' for their excellent support at sea. Thanks are also given to two anonymous referees whose comments notably improved an earlier version of this manuscript. S. Barquero, E. Teira and B. Mouriño were supported by research studentships of the Spanish Ministry of Science and Education, R. Sánchez was supported by a research fellowship of the Instituto Español de Oceanografía and A. García by a research fellowship of the Fundación Marcelino Botín. C. García-Soto acknowledges a postdoctoral contract RAMON Y CAJAL from the Ministry of Science and Technology (MCyT) of Spain. This investigation is a contribution of the research programme GIGOVI, funded by the Spanish Ministry of Education and Science (C.I.C.Y.T. MAR96-1872-CO3)

REFERENCES

Angel, M.V., Fasham, M.J., 1983. Eddies and biological processes. In: *Eddies in marine science* (ed A.R. Robinson), pp. 492–524. Berlin: Springer-Verlag.

Barnes, S.L., 1964. A technique for maximizing details in numerical weather map analyses. *Journal of Applied Meteorology*, **3**, 396–409.

Barnes, S.L., 1973. Mesoscale objetive map analysis using weighted time series observations. NOAA Tech. Memo. ERL NSLL-62. 60 pp. [NTIS COM-73-10781]

Dickson, R.R., Hughes, D.G., 1981. Satellite evidence of mesoscale eddy activity over the Biscay abyssal plain. *Oceanologica Acta*, **4**, 43–46.

Dugdale, R.C., Goering, J.J., 1967. Uptake of new and regenerated forms of nitrogen in primary productivity. *Limnology and Oceanography*, **12**, 196–206.

Falkowski, P.G., Ziemann, D., Kolber, Z. Bienfang, P.K., 1991. Role of eddy pumping in enhancing primary production in the ocean. *Nature*, **352**, 55–58.

Fernández, E., Bode, A., 1994. Succession of phytoplankton assemblages in relation to the hydrography in the southern Bay of Biscay: a multivariate approach. *Scientia Marina*, **58**, 191–205.

Flierl, G.R., 1977. The application of linear quasigeostrophic dynamics to Gulf Stream Rings. *Journal of Physical Oceanography*, **7**, 365–379.

Fraser, J.H., 1968. Standardization of zooplankton sampling methods at sea. In: *Monographs on oceanographic methodology, (2): Zooplankton sampling*. UNESCO: Paris. 174 pp.

García-Soto, C., Pingree, R.D., Valdés, L., 2002. Navidad development in the Southern Bay of Biscay: climate change and swoddy structure from remote sensing and *in situ* measurements. *Journal of Geophysical Research*, **107**, 101029.

García-Soto, C., 2004. Prestige oil spill and Navidad flow. *Journal of the Marine Biological Association of the UK*, **84**, 297–300.

García-Soto, C., Pingree, R.D., Valdés, L., 2002. Navidad development in the Southern Bay of Biscay: Climate change and swoddy structure from Remote Sensing and *in situ* measurements. *Journal of Geophysical Research*, **107** (C8), 10.029/2001JC001012.

Garçon, V.C., Oschlies, A., Doney, S.C., McGillicuddy, D., Waniek, J., 2001. The role of mesoscale variability on plankton dynamics in the North Atlantic. *Deep-Sea Research* **48**, 2199–2226.

Glibert, P.M., Lipschultz, F., McCarthy, J.J., Altabet, M.A., 1982. Isotope dilution models of uptake and remineralization of ammonium by marine plankton. *Limnology and Oceanography*, **27**, 639–650.

Gould, R.W., Fryxell, G.A., 1988. Phytoplankton species composition and abundance in a Gulf Stream warm core ring. II. Distributional patterns. *Journal of Marine Research*, **46**, 399–428.

Grasshoff, K., Erhardt, M., Kremling, K., 1983. *Methods of seawater analysis*. 2nd. edn. Verlag Chemie: Weinheim, 419 pp.

Holligan, P.M., Aarup, T., Groom, S.B., 1989. The north sea satellite colour atlas. *Continental Shelf Research*, **9**, 667–765.

Jeffrey, S.W., Hallegraeff, G.M., 1980. Studies of phytoplankton species in a warm core eddy of the East Australian Current. 1. Summer populations. *Marine Ecology Progress Series*, **3**, 285–294.

Jenkins, W.J., 1988. Nitrate flux into the euphotic zone near Bermuda. *Nature*, **331**, 521–522.

Joyce, T.M., Backus, R., Baker, K., Blackwelder, P., Brown, O., Cowles, T., Evans, R., Fryxell, G., Mountain, D., Olson, D., Schlitz, R., Schmitt, R., Smith, P., Smith , R., Wiebe, P., 1984. Rapid evolution of a Gulf Stream warm-core ring. *Nature*, **308**, 837–840.

Krom, M.D., Brenner, S., Kress, N., Neori, A., Gordon, L.I., 1992. Nutrient dynamics and new production in a warm-core eddy from the eastern Mediterranean Sea. *Deep-Sea Research*, **39**, 467–480.

Le Traon, P.Y., and Ogor, F., 1998. ERS-1/2 orbit error improvement using TOPEX-Poseidon: The 2 cm challenge. *Journal of Geophysical Research*, **103**, 8045–8057.

Madelain, F., Kerut, E.G., 1978. Evidence of mesoscale eddies in the Northeast-Atlantic from a drifting buoy experiment. *Oceanologica Acta*, **1**, 159–168.

McGillicuddy, D.J., Robinson, A.R. 1997. Eddy-induced nutrient supply and new production in the Sargasso Sea. *Deep-Sea Research*, **44**, 1427–1450.

McGillicuddy, D.J., Robinson, A.R., Siegel, D.A., Jannasch, H.W., Johnson, R., Dickey, T.D., McNeil, J.M., Michaels, A.F., Knap, A.H., 1998. Influence of mesoscale eddies on new production in the Sargasso Sea. *Nature*, **394**, 263–266.

McGillicuddy, D.J., Johnson, R., Siegel, D.A., Michaels, A.F., Bates, N.R., Knap, A.H., 1999. Mesoscale variations of biogeochemical properties in the Sargasso Sea. *Journal of Geophysical Research* **104**, 13381–13394.

Mouriño, B., Fernández, E., Escánez, J., De Armas, D., Giraud, S. Sinha, B. Pingree, R., 2002. A SubTropical Oceanic Ring of Magnitude (STORM) in the Eastern North Atlantic: physical, chemical and biological properties. *Deep-Sea Research*, **49**, 4003–4021.

Nelson, D.M., Duclow, H.W., Hitchcock, G.L., Brzezinski, M.A., Cowles, T.J., Garside, C., Gould, R.W., Joyce, T.M., Langdon, C., McCarthy, J.J., Yentsch, C.S., 1985. Distribution and composition of biogenic particulate matter in a Gulf Stream warm-core ring. *Deep-Sea Research*, **32**, 1347–1369.

Norland, S. Heldal, M., Tumyr, O., 1987. On the relation between dry matter and volume of bacteria. *Microbial Ecology*, **13**, 95–101.

Oschlies, A., Garcon, V., 1998. Eddy-induced enhancement of primary production in a model of the North Atlantic Ocean. *Nature*, **394**, 266–269.

Oschlies, A., Koeve, W., Garcon, V., 2000. An eddy-permitting coupled physical–biogeochemical model of the North Atlantic, 2, Ecosystem dynamics and comparison with satellite and JGOFS local studies. *Global Biogeochemical Cycles*, **14**, 499.

Pingree, R.D., 1984. Some applications of remote sensing to studies in the Bay of Biscay, Celtic Sea and English Channel. In: *Remote sensing of shelf seas hydrodynamics, Proceedings of the 15th International Liège Colloquium on ocean hydrodynamics* (ed. J.C.J. Nihoul), pp. 287–315. Amsterdam. Elsevier.

Pingree, R.D., Le Cann, B., 1990. Structure, strength and seasonality of the slope currents in the Bay of Biscay region. *Journal of the Marine Biological Association of the United Kingdom*, **70**, 857–885.

Pingree, R.D., Le Cann, B., 1992a. Three anticyclonic slope water oceanic eddies (SWODDIES) in the southern Bay of Biscay. *Deep-Sea Research* **39**, 1147–1175.

Pingree, R.D., Le Cann, B., 1992b. Anticyclonic eddy X91 in the southern Bay of Biscay, May 1991 to February 1992. *Journal of Geophysical Research*, **97**, 14353–14367.

Pinot, J.M., Tintoré, J., López-Jurado, J.L., Fernández de Puelles, M.L., Jansa, J., 1995. Three-dimensional circulation of a mesoscale eddy/front system and its biological implications. *Oceanologica Acta*, **18**, 389–400.

Porter K.G., Feig Y. S., 1980. The use of DAPI for identifying and counting aquatic microflora, *Limnology and Oceanography* **25**, 943–948.

Redfield, A.C., Ketchum, B.H., Richards, F.A., 1963. The influence of organisms on the composition of sea-water. In: *The sea*, Vol. 2 (ed. M.N. Hill), pp. 26–79. New York: Wiley Interscience.

Rodríguez, F., Varela, M., Fernández, E., Zapata, M., 2003. Phytoplankton and pigment distributions in an anticyclonic slope water oceanic eddy (SWODDY) in the southern Bay of Biscay. *Marine Biology*, **143**, 995–1011.

Author: col 1 García-Soto 2002 et al. please check page range

Rodríguez, J., Tintoré, J., Allen, J.T., Blanco, J.M., Gomis, D., Reul, A., Ruiz, J., Rodríguez, V., Echevarría, F., Jiménez-Gómez, F., 2001. Mesoscale vertical motion and the size structure of phytoplankton in the ocean. *Nature*, **410**, 360–363.

Sahlsten, E., 1987. Nitrogenous nutrition in the euphotic zone of the Central North Pacific Gyre. *Marine Biology*, **96**, 433–439.

Sánchez, F., Gil, J., 2000. Hydrographic mesoscale structures and Poleward Current as a determinant of hake (*Merluccius merluccius*) recruitment in southern Bay of Biscay. *ICES Journal of Marine Science*, **57**, 152–170

Sánchez, R., Gil, J., Structure, mesoscale interactions and potential vorticity conservation in a 3D Swoddy in the Bay of Biscay. *Journal of Marine Systems*. In press.

Serret, P., Fernández, E., Sostres, J.A., Anadón, R., 1999. Seasonal compensation of microbial production and respiration in a temperate sea. *Marine Ecology Progress Series*, **187**, 43–57.

Siegel, D.A., McGillicuddy, D.J., Fields, E.A., 1999. Mesoscale eddies, satellite altimetry, and new production in the Sargasso Sea. *Journal of Geophysical Research*, **104** (C6), 13359–13379.

Smith, C.L., Richards, K.J., Fasham, M.J., 1996. The impact of mesoscale eddies on plankton dynamics in the upper ocean. *Deep-Sea Research*, **43**, 1807–1832.

Teira, E., Serret, P., Fernández, E., 2001. Phytoplankton size-structure, particulate and dissolved organic carbon production and oxygen fluxes through microbial communities in the NW Iberian coastal transition zone. *Marine Ecology Progress Series*, **219**, 65–83.

The Ring Group, 1981. Gulf Stream cold-core rings: their physics, chemistry and biology. *Science*, **212**, 1091–1100.

Tranter, D.J., Parker, R.R., Cresswell, G.R., 1980. Are warm-core eddies unproductive?. *Nature*, **284**, 540–542.

UNESCO, 1994. Protocols for the Joint Global Ocean Flux Study (JGOFS) core measurements. *Manuals and Guides* **29**, 1–170.

Varela, R.A., Figueiras, F., Agustí, S., Arbones, B., 1998 Determining the contribution of pigments and the non-algal fraction to total absorption: towards a global algorithm. *Limnology and Oceanography* **43**, 449–457.

Wyrtki, K., Magaard, L., Hager, J., 1976. Eddy energy in the oceans. *Journal of Geophysical Research* **81**, 2641–2646.

Yamamoto, T., Nishizawa, S., 1986. Small-scale zooplankton aggregations at the front of a Kuroshio warm-core ring. *Deep-Sea Research*, **33**, 1729–1740.

Zapata, M., Rodríguez F., Garrido, J.L., 2000. Separation of chlorophylls and carotenoids from marine phytoplankton: a new HPLC method using reversed phase C_8 column and pyridine-containing mobile phases. *Marine Ecology Progress Series*, **195**, 29–45.

Submitted ●●●. *Accepted* ●●●.